

ЗАГАЛЬНІ ПИТАННЯ ТЕОРІЇ ТЕРТЯ ТА ЗНОШУВАННЯ

УДК 621.315.592:621.91:620.181

*A. M. Kovalchenko, Candidate of Technical Sciences
Senior Researcher*

A REVIEW OF STUDIES REGARDING DUCTILE REGIME MACHINING OF SEMICONDUCTORS, CERAMICS AND GLASS

Institute for Problems of Materials Science
National Academy of Science of Ukraine

A review considers the emerging treatment method, the ductile regime machining of brittle materials such as semiconductors, ceramics, glasses, etc. to achieve smooth surfaces with minimum defects. The ductile mode is connected with implementation phase transformations (metallization or amorphization) that occur in brittle materials under such contact loading as indentation, scratching, friction, grinding and cutting. The review observes theoretical and experimental studies. It was shown that the tool cutting edge radius, undeformed chip thickness, tool rake angles, crystallographic orientation, cutting lubricants and some others parameters are critical for maintaining the ductile mode.

The application of brittle materials in various fields of modern industry such as semiconductors, ceramics, glasses, etc. has led to development of processing technologies of these materials. The most widely used brittle material is single-crystal silicon, which is not only a dominant substrate material for the fabrication of integrated circuits, micro-electro and mechanical components but also an important infrared optical material.

Silicon processing has become an emerging technology of the twenty-first century. As a substrate material used in microelectronic chips, silicon wafer requires flatness and good surface integrity. Usually, silicon substrates are manufactured by mechanical machining processes such as slicing, cutting and grinding. In this manufacturing procedure, because cutting and grinding is a somewhat random and uncontrolled material removal process, brittle fracture and severe subsurface damage of the silicon wafers are inevitable. Consequently, the surface left by the grinding operation cannot be used directly for further applications and post-grinding operations, such as lapping, edge profiling and

chemo-mechanical polishing, are usually needed to enable the wafer to achieve a high-quality surface. This manufacturing procedure of silicon wafers is complicated, time-consuming, and costly. In order to overcome the problems in the current manufacturing procedure of silicon wafer to replace in some extent the grinding, lapping, and polishing operations, a new technology, ductile mode cutting, has been proposed and intensively studied around the world. Using ductile regime, silicon and other brittle materials could be deformed plastically in ultra-precision cutting, without cracking, yielding ductile chips. Very smooth surface quality can be obtained. The schemes of the ductile mode cutting, in comparison with traditional cutting of brittle materials are shown in fig. 1.

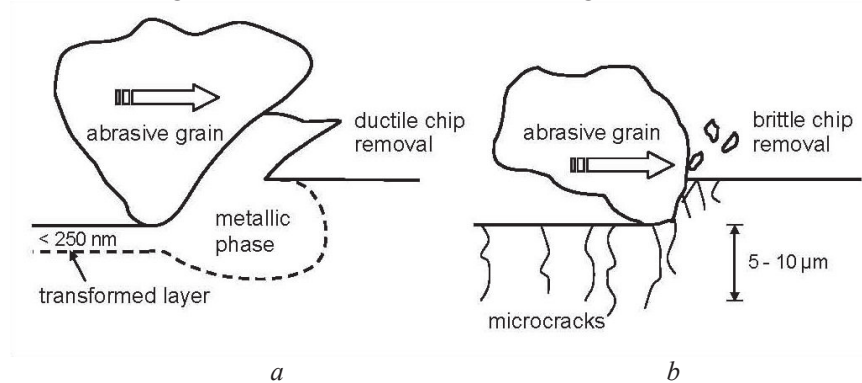


Fig. 1. Schematics of the two regimes of abrasive machining; (a) ductile mode removal of material via pressure-induced metallization in the surface layer and (b) brittle fracture [25]

The possibility of grinding brittle materials in a ductile manner was proposed by King and Tabor [1] (1954), when it was noted that during frictional wear of rock salts, although there was some cracking and surface fragmentations, the dominant material removal process was plastic deformation of the surface layers and not fracture. Huerta and Malkin [2] (1976) showed first reproducible evidence of grinding brittle glass workpieces with the improvements in precision diamond grinding mechanisms at that time. At present, as the papers [3; 4] report, the demand for precision parts made of silicon, glass and advanced ceramics obtained by ductile or partial ductile mode machining are increasing at a first rate. However, much needs to be determined in respect of the cutting conditions to enable this ductile behavior to be successfully main-

tained throughout the machining processes such as turning or grinding. Despite some articles presents fine grinding of silicon wafers, demonstrating the importance of choosing the correct grinding parameters and development of new machining processes that have the precision and control required to achieve the necessary levels of surface integrity [5–10], reduced polishing time and improved surface quality with extremely flat crack-free mirror surfaces can be realized mainly with the implementation of ductile regime grinding [11].

An ability to perform single point diamond turning of poly crystal silicon carbide was demonstrated in [12]. It was believed that the ductility of SiC during machining is due to the high-pressure phase at the cutting edge of the tool, which encompasses the chip formation zone. As the authors remark, this phase transformation mechanism is similar to that found with other semiconductors and ceramics, leading to a plastic response rather than brittle fracture at small size scales. In contrast [13], the x-ray diffraction indicated that no phase transformation in silicon carbide occurred during the ductile regime mode grinding. Laboratory-scale ductile-regime fixed-abrasive grinding of chemically vapor deposited silicon carbide is described in [14]. It was shown that ductile grinding of ceramic substrates can produce optical quality surfaces. The paper [15] presents research results on ultraprecision machining of metal matrix composite composed of aluminum matrix and either SiC or Al_2O_3 particles. Ductile-regime machining was evaluated to improve the surface integrity.

Series of papers proposes new treatment methods of brittle materials to achieve smooth surfaces with minimum defects. A ductile-machining numerically controlled system based on the straight-line enveloping method was developed [16; 17] for fabricating aspheric surfaces on hard brittle materials. By adopting a small angle between the cutting edge and the tangent of the objective surface, this method enables the uniform thinning of the undeformed chip thickness to the nanometric range, and thus provides complete ductile regime machining of brittle materials. The paper [18] reports on the development of a machining device, which is capable of carrying out precision machining experiments under externally applied hydrostatic pressure. Machining trials were conducted on hard-brittle materials such as soda glass, quartz glass, silicon and quartz wafers. The applied hydrostatic pressure en-

hanced the critical cross sectional area and reduced the cracks and chip-pings of all the tested materials. The mechanism behind the enhancement of ductile-brittle transition by the externally applied hydrostatic pressure is also elucidated by a theoretical model. The papers [19; 20] address the effects of bonds and grains of abrasive tools on semi-ductile mode of grinding. Diamond grains and SiC grains combined with two bond types, i.e., resin and metal were considered for the study. However, using a resin-bonded wheel, two mechanisms of material removal were revealed according to grains' type. A partial ductile regime, i.e., ductile streaks and brittle fracture were obtained with diamond grains, and a fully ductile regime was obtained with SiC grains. Thus, it was found that ground surface obtained using SiC grains' wheel has a better roughness than that obtained using diamond grains wheel. Besides, SiC grains seem to lead to more marked streaks and form defects. The effect of finish electrolytic in-process dressing (ELID) grinding using different grit sized metal bonded diamond grinding wheels on the flexural strength of silicon nitride specimens were studied in the investigations [21–22]. A significant improvement in the strength of the Si_3N_4 specimens was noted and mirror surface finish was realized when finish ELID grinding was performed. This was the result that material was predominantly removed in the ductile mode as SEM and AFM studies reveal. New approach to polish silicon wafers was proposed in the studies [23; 24], where nanoabrasives were bonded by ice to make ice bonded fixed abrasive pads (IFA) and the wafer was polished with the IFA under cryogenic conditions. Abrasive slurry was made of nano-sized Al_2O_3 and CeO_2 particles dispersed in de-ionized water with a surfactant and the slurry was frozen to form an ice-polishing pad. The results show that a supersmooth surface with roughness of $R_a=0,3-0,56$ nm were obtained. No microcracks are found in the subsurface of the workpiece. The removal of material is dominated by the coactions of ductile regime machining and chemical corrosion.

The review [25] provides an analysis of phase transformations and amorphization that occur in silicon under contact loading, such as indentation with hard indenters, scratching or different machining processes like dicing, slicing, grinding, polishing. As the example of the metallization of the typically brittle material, the fig. 2, *a-c* show SEM micrographs if the indentation in silicon revealing plastically extruded materials. The authors stress that the processes of phase transformations

have only been investigated for a very few materials (silicon is one of them) and further research is necessary. One of the reasons for the lack of information may be the fact that the problem is at the interface between at least three scientific fields, that is, materials science, mechanics, and solid-state physics. Thus, an interdisciplinary approach is required to solve this problem and understand how and why a hydrostatic or shear stress in the two-body contact can drive phase transformations in materials.

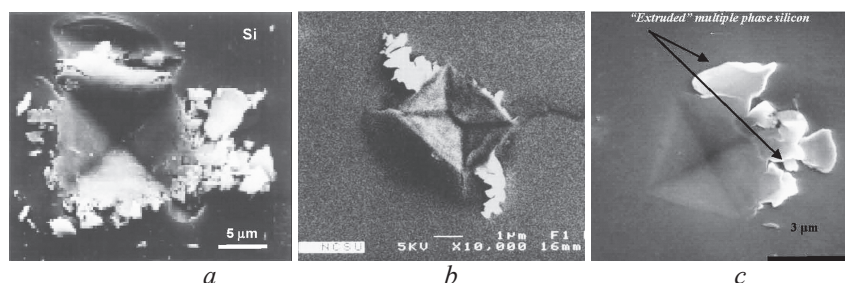


Fig. 2. Scanning electron micrographs (SEM) of indentation in silicon revealing plastically extruded material. The sources of the images (a) – [25], (b) – [31] and (c) – [34]

A germanium surface and the chips produced from a single-point diamond turning process operated in the "ductile regime" have been analyzed by transmission electron microscopy and parallel electron-energy-loss spectroscopy in the early (1995) study [26]. Lack of fracture damage on the finished surface and continuous chip formation are indicative of a ductile removal process. An energy scaling brittle-ductile transitions in machining of silicon by diamond was presented in [27] (1995). Surfaces were profiled by AFM and subsurface damage was characterized by Rutherford ion backscattering and cross section TEM. The main results to date are that specimens possessed a surface quality corresponding to that achieved by optical polishing after highly stiff single point diamond turning using cut depths of the order of 100 nm. The R_a values of the ground specimens ranged between 7 nm and 20 nm after high precision cup grinding using a nominal cut depth of 500 nm. Also, there were significant differences between wheels bonded by resin and by cast iron. The papers [28–30] present the observation of nanoindentations made on ultraprecision diamond-turned silicon wafers and the results were compared with those of pristine silicon wafers. Remarkable differences were found

between the two kinds of test results in terms of load-displacement characteristics and indent topologies. The machining-induced amorphous layer undergoes significant plastic flow and was found to have lower hardness than pristine silicon. This work indicated the feasibility of detecting the presence and the mechanical properties of the machining-induced amorphous layers by nanoindentation.

Raman spectroscopy gains the most popularity as an effective method to detect a presence of amorphous material and residual tensile strains [25; 31–37]. As early as in 1996 the Raman spectroscopy indicated the pressure-induced transformation to metallic silicon that occurs during controlled slow-speed microcutting [31] and the ductile metallic phase facilitate the material removal process. Structural disorder and strain effects in ductile-regime single-point-diamond-turned gallium arsenide monocrystalline samples were probed by Raman scattering in [32]. A residual compressive stress of about 1,5 GPa was observed in the machined samples. This residual strain was attributed to the hysteresis of phase transformation generated by the high pressure imposed by the cutting tool tip during the machining process. Laser micro-Raman spectroscopy was used in [33] to examine the silicon substrates machined by single-point diamond turning at machining scales ranging from 10 to 1000 nm under plane strain conditions. The results showed that the subsurface layer was partially transformed to amorphous, the extent of amorphization depending strongly on the undeformed chip thickness. The intensities of the crystalline phase and the amorphous phase show opposite tendencies with respect to the undeformed chip thickness. The intensity of the amorphous phase reaches maximum near the ductile-brittle transition boundary. In ductile regime machining, the intensity of the amorphous phase decreased sharply as the undeformed chip thickness decreased. Continuous chips removed by single point ultraprecision diamond turning of single crystal silicon have been investigated by means of SEM/TEM and micro-Raman Spectroscopy [34–38]. The damage found is characterized by an amorphous phase in the outmost surface layer. Specifically [35], it was reported for the first time, the results of in-situ recrystallization annealing of micromachined silicon. Silicon also has been diamond turned under different cutting conditions in [38]. Compressive residual stresses are estimated for the machined surface and it is observed that they decrease with an increase in the feed rate and depth of cut. This

behavior has been attributed to the formation of subsurface cracks when the feed rate is higher than or equal to $2.5 \mu\text{m/rev}$. The surface roughness was observed to vary also with cutting conditions alteration.

Silicon probe tips are used widely in micro and nano-systems such as AFM, MEMS as well as in other probe-based applications. The wear and mechanical integrity of the tip is important to assure reliable performance of the tip during loading and sliding contacts. Silicon tip wear tests under extremely low normal load were conducted in order to understand the nature of wear [39]. It was found that fracture of the tip readily occurred due to impact during the approach process. Experimental results showed that the impact should be below 0.1 nN to avoid significant fracture of the tip. Astoundingly, it was observed that wear of the amorphous layer, formed at the end of the tip, occurred at the initial stage of the silicon tip damage process. In the work [40], the silicon probe tip deformation process during nano-indentation and scribing was investigated by using molecular dynamics simulation to observe the frictional characteristics of crystalline and amorphous silicon structures. The results showed that the structure of silicon near the surface was permanently deformed at a contact stress of approximately 17 GN/m^2 . It was also found that the atomic structure of the silicon tip in the contact region affected the frictional behavior.

The model scratch tests have been performed in [41–43] to determine the transition of material removal from brittle to ductile. Influence of applied loads and diamond tools [41] (Vickers, sharp conical, and spherical Rockwell indentors) were studied to reveal the critical depth of cut or penetration depth for the transition. Scratch resistance of the single silicon wafer after ice polishing was used in [23] to explore the mechanical removal mechanism. The papers [44; 45] deal with material removal mechanisms of single-crystal silicon [44], as well as amorphous silicon and borosilicate [45] on nanoscale and at ultralow loads. Acoustic emission is proposed in [46–47] as a means of monitoring the ductile to brittle transition, and thereby predict surface quality in microindentation and microscratching of single crystal silicon [46], CVD silicon carbide and quartz [47]. A method of in-situ infrared detection of the high-pressure phase transformation of silicon during dead-load scratching is described in [48]. The method is based on the simple fact that single crystal silicon is transparent to infrared light while metallic materials

are not. As presented in [49], scratch tests on single crystal silicon under dry sliding and pentadecane lubrication are performed on a commercially available nano-scratch tester. Based on the results obtained, a simple approach to fabricate amorphous silicon pattern on single crystal silicon is introduced and discussed. In the papers [50–51], a similar friction-induced nanofabrication method is proposed to fabricate protrusive nanostructures on silicon, which is completed by sliding an AFM diamond tip. Finalizing the consideration of the scratch tests, it should be noted that these experiments simulate in nano- and micro-levels a plunge-cut approach to investigate the ductile-to-brittle transition in monocrystalline silicon proposed by Brinksmeier [52] in 1998. Schematic of the four different regimes of material response in a plunge-cut made in monocrystalline silicon is shown in fig. 3.

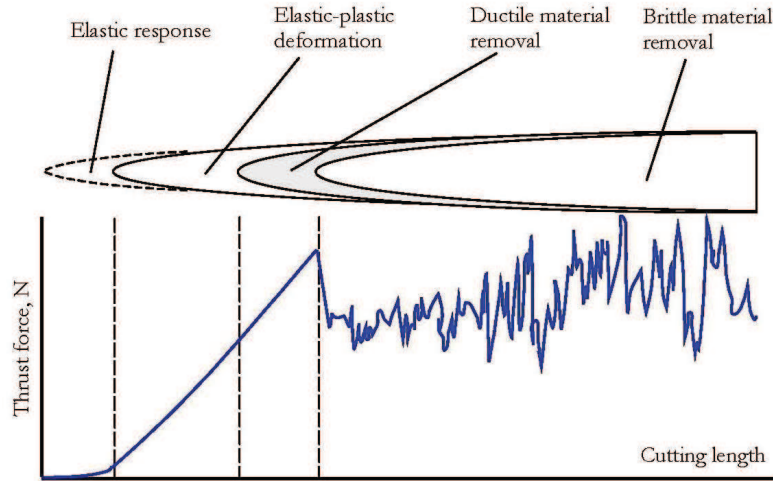


Fig 3. Schematic of the four different regimes of material response in a plunge-cut made in monocrystalline silicon after Brinksmeier et al [52]

The elastic response regime is governed by a steady increase in the thrust force without any trace of surface damage (fig. 3). In the elastic-plastic regime, the thrust force continues to increase, but without visible change in surface topography. As the tool approaches the ductile-to-brittle transition, the thrust force reaches a local maximum. In the brittle regime, the thrust force per unit volume of material removed decreases with random variations in the force caused by the fracture process.

Papers [53; 54] consider ductile regime machining of brittle materials is due to the joined influence of a thermal and a mechanical effect. The authors stressed that mechanical influences in ductile mode machining have received considerable attention due to the relative facility by which the mechanical behavior can be characterized. Thermal influences, however, were not the subject of many investigations due to the difficulties encountered in monitoring the thermal behavior of the ductile silicon phase. The papers [53; 54] reports on a series of micro-scratching experiments that were designed to remedy the current gap. The experiments mimic ductile machining by scratching the surface of single crystal silicon wafers using a stylus with spherically capped diamond tip. In situ electrical resistivity measurements of the wafer surface allowed monitoring the behavior of silicon in the ductile regime, electrical resistivity measurements were teamed to temperature computations. Applying the Wiedemann-Franz-Lorentz law, thermal conduction fields in the wafers characterized. As such, the thermal environment in the workpiece-stylus contact zone during the brittle-ductile transformation was characterized. The results indicate that: while covalent silicon is an average thermal conductor ($K = 120\text{--}124 \text{ W/mK}$), the ductile phase is rather insulative (K approximate to $1\text{--}2,5 \text{ W/mK}$).

Some articles deal with phase transformation occurred during friction experiments. The tribological behaviors and phase transformations of single-crystal silicon against Si_3N_4 at room temperature were investigated in [55–56]. SEM and Raman analysis indicate that phase transformation was involved especially in the early stage at the low velocity at dry sliding and at lubricating conditions. The plastically deformed layer was wiped off at high-velocity or long sliding duration at dry conditions. Boundary lubrication permits continuously to retain phase transformation and plastically deformed layer on surface. Plastic flow of phase-transformed amorphous Si layer is shown in fig. 4. Phase transformation behaviors of silicon lubricated by different fluids were investigated in [57]. Surface analyses indicated that two major factors including viscosity and hydrogen bond of lubricant influence the phase transformation of single crystal silicon, and only the lubricant with relative high viscosity and weak hydrogen bond facilitates the phase transformation. As a result, pentadecane could be selected as a suitable lubricant to fabricate a smooth amorphous silicon surface.

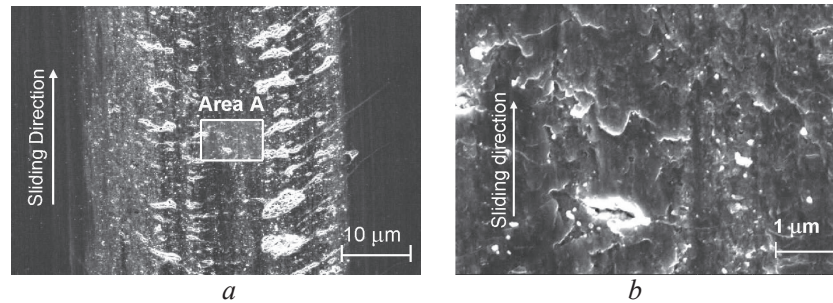


Fig. 4. SEM images of wear track on silicon after friction in air against Si_3N_4 counterface. (a) – general view, (b) – fragment; area of amorphous plastic flow (Area A on fig. 4, a) [55]

The friction of silicon against Si_3N_4 , Ruby and steel were investigated in [58]. It was found that the strong chemical action between silicon and Fe was the key factor to the tribological behavior of silicon as slid against steel. SEM and Raman spectroscopy indicated that phase transformation of silicon occurred as slid against Si_3N_4 and Ruby. As the conclusion, the high hardness of counterpart and the absence of chemical action between silicon and counterpart facilitated the phase transformation of single crystal silicon.

In order to understand physical essence of ductile machining process, molecular dynamics (MD) simulations have been conducted in numerous following referred studies. The results show [59–63] that huge hydrostatic pressure induced in the local area leads to the silicon atom transform from classical diamond cubic structure (alpha silicon) to metal six-coordinated silicon (beta silicon) and amorphous phase. At the same time, the stress concentration is avoided by uniformly distributed pressure in the cutting area. These two important factors together result in the ductile machining of silicon and then acquire super-smooth surface. During phase transformation, atoms are of high potential and temperature, and the values of pressure and temperature are in good agreement with those according to the phase diagram. In [64], an atomic dynamic model is proposed, where crack propagation in nanoscale ductile mode cutting of silicon wafer is screened by a large compressive stress such that chip formation is dominated by dislocation emission rather than crack propagation. The articles discuss [65; 66] the ductile response of semiconductors crystals based on the quantitative dependence of brittle-to-ductile transition upon the transition pressure value in single

point diamond turning when appropriate cutting conditions are applied. This was investigated by carrying out microindentation and single point diamond turning tests in three different (001)-oriented semiconductors; InSb, GaAs and Si single crystals. It is shown that the transition pressure value can be considered as a useful information to predict whether the ductile or brittle regime will prevail during micromachining and consequently to determine the machinability of monocrystalline semiconductor crystals. It is proposed that the ductility of semiconductors crystals during machining is inversely proportional to the transition pressure value. The submicron-level orthogonal cutting process of silicon has been investigated by the finite element approach, and the effects of tool edge radius on cutting force, cutting stress, temperature and chip formation were investigated in [67]. The results indicate that increasing the tool edge radius causes a significant increase in thrust force and a decrease in chip thickness. A hydrostatic pressure (similar to 15 GPa) is generated in the cutting region, which is sufficiently high to cause phase transformations in silicon. The volume of the material under high pressure increases with the edge radius. The simulation results from the study could successfully explain existing experimental phenomena. In the work [68], the mechanical behavior of silicon nitride machined in ductile fashion under high pressures and at low depths of cut is treated using the Drucker-Prager yield criterion implemented in the commercial machining software AdvantEdge. Numerical simulations are carried out for depths of cut ranging from 1 to 40 μm and at cutting speeds ranging from 25 to 300 m/min. The parametric study shows that, when the depths of cut are small, the pressure in the workpiece approaches the hardness value of silicon nitride in the region near the workpiece-tool interface, indicating that material transition to ductile mode occurs in this region.

For a better understanding of essential mechanisms of material removal at extremely small depth of cut and of the brittle-ductile transition in the material removal process of monocrystalline silicon, nanometric deformation behavior in three-point bending of defect-free monocrystalline silicon is analyzed by molecular dynamics simulation in the study [69]. The simulations show that plastic deformation takes place through a phase transformation from diamond to amorphous structures. The critical octahedral shearing stress for phase transformation is estimated to be 12 – 14 GPa. In the deformed region, a crack nucleus on atomic scale can be generated owing to thermally activated vibration of

atoms. After the crack nucleus, the crack extension takes place under a certain stress field. The crack initiation takes place when a tensile stress reaches a certain critical value of about 30 GPa at the crack nucleus. The critical values for plastic deformation and crack initiation depend on crystal orientation and hydrostatic pressure. It is shown that there can also be critical criteria of the stress field to determine whether plastic deformation or crack initiation would predominantly take place. When the plastic deformation proceeds to a crack initiation, ductile mode machining can be realized.

Results in [70] show that amorphous phase transformation of silicon is a key mechanism for inelastic deformation, and stable shearing of the amorphous phase is necessary for ductile-mode machining which was obtained by molecular dynamics simulation for ductile-mode machining, nano-indentation, nano-bending, and nano-machining of defect-free mono-crystalline silicon. Stress analysis suggests that stable shearing takes place under a compressive stress field. In practice, a sharp cutting edge tool with a large negative rake angle should be used for effective ductile-mode machining, and vibration machining should be applied for larger depths of cut as it enlarges the amorphous region in front of the cutting edge. Molecular dynamics method also has been developed in the study [71] for a simulation system for nanoscale ductile mode cutting of monocrystalline silicon using for the better understanding of the ductile mode cutting mechanism. In this model, the initial atom positions of silicon workpiece material are arranged according to the crystal lattice structure, the atomic interactive actions of silicon are based on the Tersoff potential, the diamond cutting tool is assumed to be undeformable, the tool cutting edge is realistically modelled to have a finite radius, and the motions of the atoms in the chip formation zone are determined by Newton's equations of motion. The simulated variation of the cutting forces with the tool cutting edge radius is compared with the results of experimental cutting tests to substantiate the developed simulation system and the results show a good agreement with analytical findings. Experimentally, the effect of cutting edge geometry, depth of cut and undeformed chip thickness on the machined surface quality was studied by actual diamond turning in [42; 72; 73] for silicon, in [74] for germanium and in [75] for CaF_2 . A sketch for subsurface damage mechanism in silicon during ductile machining is shown in fig. 5 [72].

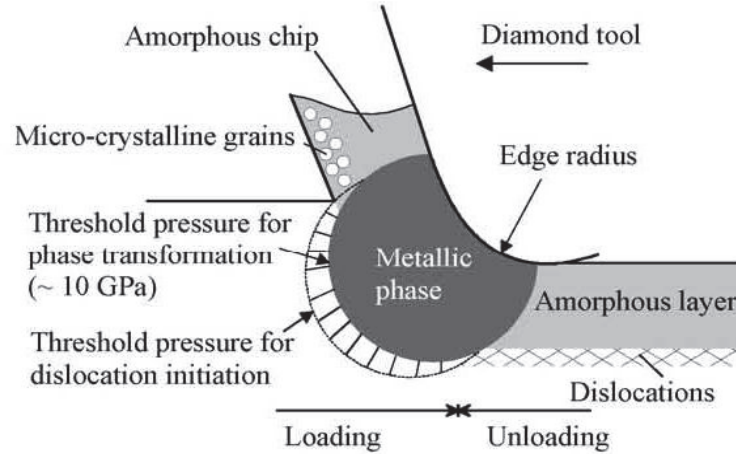


Fig. 5. Schematic model for subsurface damage mechanism in silicon during ductile machining [72]

The results showed that it was possible to produce uniformly ductile-cut surfaces and amorphous debris by using an extremely small undeformed chip thickness (in the range of 50–100 nm) under negative tool rake angles (similar to -45°). The results of monocrystalline silicon micro-drilling [76] showed that ductile-regime cutting was realized and the fractures at the hole entrance is prevented if a depth of cut is less than $0.1\text{ }\mu\text{m}$, and a tool clearance angle is larger than 0 .

According to the experimental results, the authors of [77] indicate that when the depth of cut in ductile-regime machining of (100) silicon wafers was of the magnitude of the tool edge sharpness, the surface finish was degraded by radial cracks in the lateral plane owing to rubbing between the tool and the workpiece. Also in [78], it was remarked that in cutting of brittle materials, it was experimentally observed that there is an upper bound of tool cutting edge radius, beyond which, although the undeformed chip thickness is smaller than the tool cutting edge radius, the ductile mode cutting cannot be achieved, and this phenomenon has not been fully understood. Thus, in the study [78], based on the tensile stress distribution and the characteristics of the distribution obtained from molecular dynamics simulation of nanoscale ductile cutting of silicon, an approximation for the tensile stress distribution was obtained. Using this tensile stress distribution with the principles of geometrical

similarity and fracture mechanics, the critical conditions for the crack initiation have been determined. The result showed that there is a critical tool cutting edge radius, beyond which crack initiation can occur in the nanoscale cutting of silicon, and the chip formation mode is transferred from ductile to brittle. That is, this critical tool cutting edge radius is the upper bound of the tool cutting edge radius for ductile mode cutting of silicon. The effect of tool edge radius as well was considered as critical on ductile machining of silicon in the earlier mentioned [67].

Blake and Scattergood as early as in 1990 [79] performed a novel interrupted-cutting test and a new model of the machining process were used to measure a critical-depth parameter studying experimentally precision machining of germanium and silicon in ductile regime. This parameter governs the transition from plastic flow to fracture along the tool nose. It was shown that the critical-depth parameter can be used to provide physical insight into the effect of various machining parameters such as tool rake angle or tool clearance angle. The papers [80–81] emphasize that to achieve ductile regime grinding of silicon wafer, a fundamental concept is the application of grain depth of cut being less than the critical cut depth. The importance of the depth of cut for ductile grinding also was pointed out in [72; 76; 77]. The transition of material removal from brittle to ductile during scratching was observed by continuously changing the cutting depth to determine the critical penetration depth in [41; 42] for Si and chemically vapor deposited coated SiC in [82]. The study [43] describes numerical simulations for the determination the critical depth of cut for Si and SiC during single point diamond turning and scratching. The experiments have shown that as the depth of cut is decreased (from 250 nm to 100 nm down to 50 nm) the material removal mechanism transitions from brittle to a ductile response, with the 50 nm cuts being dominated by ductile events. The supplementary cutting tests were performed to display an agreement with the simulation.

The mentioned above sources [73; 75; 78] designate the critical value of undeformed chip thickness as the necessary parameter for the ductile mode cutting can be achieved. Its value should be smaller than the tool cutting edge radius. The paper [77] indicates that a ductile-regime was achieved when machining along the $\langle 110 \rangle$ directions of silicon crystal and the maximum chip thickness of less than 0,5 μm . Results of [83] show that the critical chip thickness in silicon for ductile material removal reaches a

maximum of 120 nm in the $\langle 100 \rangle$ direction and a minimum of 40 nm in the $\langle 110 \rangle$ direction. The minimum critical undeformed chip thickness was approximately 60 nm of single-crystal germanium [84] and 80 nm of polycrystalline germanium [74]. The minimum critical chip thickness of single-crystal calcium fluoride (CaF_2) was 85 nm [85]. The studies [86; 87] proposed a predictive model to determine the undeformed chip thickness in micro-machining in ductile manner of single crystal brittle materials. The comprehensive model includes a force model considering the rounded tool edge radius effect and ploughing. Irwin's model for computing the stress intensity factor is adopted here as it gives a relation between the stress intensity and applied normal stress including effects of crack size and crack inclination. The occurrence of plastic deformation is built upon the condition that the shear stress in the chip formation region must be greater than the critical shear stress for chip formation and the stress intensity factor must be less than the fracture toughness of the material. The point of transition takes place when the fracture toughness is equal to the stress intensity factor. These conditions form the theoretical basis for the proposed model in determining the transition undeformed chip thickness.

Ductile-regime material removal leads to the specific chip formation. In the paper [88], the research to understand the chip formation mechanism was conducted. An analysis was performed to discover how the chips are removed during the micro-end-milling process of single-crystal silicon. Forces generated when milling single-crystal silicon are used to determine the performance of the milling process. Experimental results show that the dependence of the cutting force on the uncut chip thickness can be well described by a polynomial function. As cutting regime becomes more brittle, the cutting force has more complex function. In the paper [37], continuous chips removed by single-point diamond turning of single crystal silicon have been investigated by means of scanning, transmission electron microscopy and micro-Raman spectroscopy. Three different chip structures were probed with the use of electron diffraction pattern; (1) totally amorphous lamellar structure, (2) amorphous structure with remnant crystalline material and (3) partially amorphous together with amorphous with remnant crystalline material. Furthermore, different silicon phases were depicted from the chips remained in the cutting tool rake face. Five different structural phases of silicon were found in the same debris. It was proposed that material re-

moval mechanisms may change along the cutting edge from shearing (yielding lamellar structures) to extrusion. Shearing results from structural changes related to phase transformation induced by pressure and shear deformation. Extrusion, yielding crystalline structures in the chips, may be attributed to a pressure drop (due to an increase in the contact area) from the tool tip towards the region of the cutting edge where the brittle-to-ductile transition occurs. From this region upwards, pressure (stress) would be insufficient to trigger phase transformation and therefore the amorphous phase would not form integrally along the chip width. It was found in [73] that chips removed from the material surface during diamond turning of single crystalline silicon wafers consist of nano needles, nano ribbons and nano fibers, the shape and size of which depend on the undeformed chip thickness and the cutting edge geometry. Electron diffraction studies showed that the needle-type chips are micro-crystalline with slight amorphization; while the nano ribbons and nano fibers have been mostly transformed into the amorphous phase. The work preliminarily demonstrated the feasibility of an efficient and inexpensive production method for mechanically flexible nano ribbons and nano fibers for micro-nano mechanical and electronic applications. The study [89] also noted that the silicon chips have amorphous structure and polycrystalline structure when the cutting is in ductile mode and brittle mode, respectively. The studies [17; 35; 38; 64; 72; 74; 85; 86] as well touch the chip formation in connection with ductile material removal. The typical SEM views of amorphous chips of Si [35; 73; 86] and CaF_2 [85] are shown in fig. 6.

The studies [64; 90–94] indicate that, according to experimental results, two conditions must be satisfied for ductile mode cutting of silicon wafer material; the cutting edge radius does not exceed a certain upper bound value, and the undeformed chip thickness is less than the cutting edge radius.

Based on the molecular dynamics simulation in [91], it is found that the critical upper bound for the cutting edge radius in the ductile mode chip formation relates to the stress condition in the cutting region. The shear stress decreases as the tool edge radius is increased. As the cutting edge radius increases beyond the limit, the insufficient shear stress will cause both surface and subsurface damage on the machined workpiece. For the cutting of silicon under the same conditions, the limit for the cutting edge radius was found to be about 807 nm, which was verified through cutting experiments in [92].

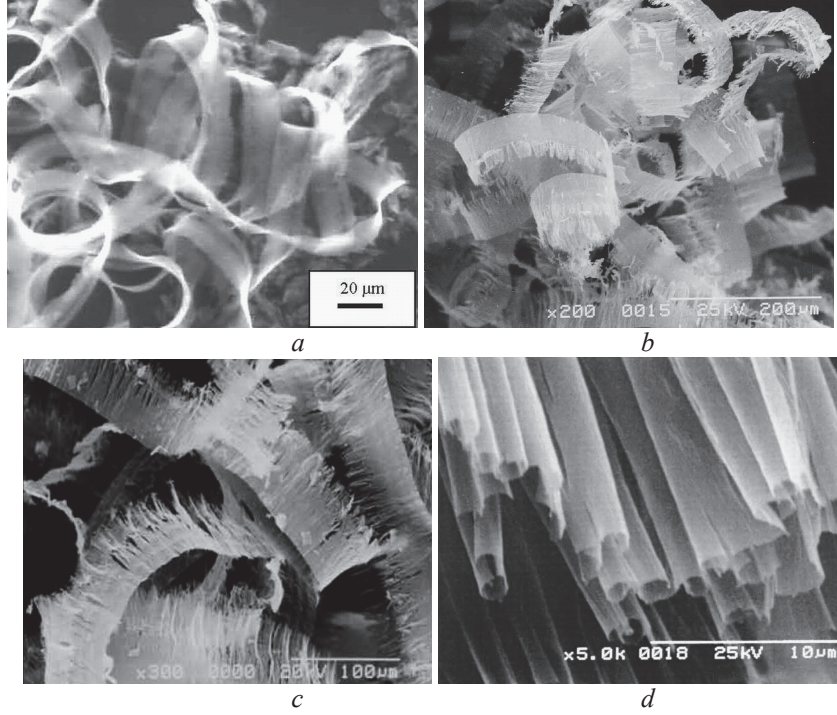


Fig. 6. The typical SEM views of amorphous chips of Si (*a-c*) [35; 73; 86] and CaF_2 (*d*) [85]

In the study [93], the molecular dynamics method is employed to model and simulate the nanoscale ductile mode cutting of monocrystalline silicon wafer. It was found that when the ductile cutting mode is achieved in the cutting process, the thrust force acting on the cutting tool is larger than the cutting force. As the undeformed chip thickness increases, the compressive stress in the cutting zone decreases, giving way to crack propagation in the chip formation zone. As the tool cutting edge radius increases, the shear stress in the workpiece material around the cutting edge decreases down to a lower level, at which the shear stress is insufficient to sustain dislocation emission in the chip formation zone, and crack propagation becomes dominating. Consequently, the chip formation mode changes from ductile to brittle. In the other study [94], the crack initiation in the ductile-brittle mode transition also has been simulated using the molecular dynamics on nanoscale cutting of

monocrystalline silicon with a non-zero edge radius tool, from which, a peak deformation zone in the chip formation zone has been found in the transition from ductile mode to brittle mode cutting. The results show that as the undeformed chip thickness is larger than the cutting edge radius, in the chip formation zone there is a peak deformation depth in association with the connecting point of tool edge and the rake face, and there is a crack initiation zone in the undeformed workpiece next to the peak deformation zone, in which the material is tensile stressed and the tensile stress is perpendicular to the direction from the connecting point to the peak. As the undeformed chip thickness is smaller than the cutting edge radius, there is no deformation peak in the chip formation zone, and thus there is no crack initiation zone formed in the undeformed workpiece.

Molecular dynamics simulations in [95] of nanometric cutting of single-crystal, were performed using the Tersoff potential over a wide range of rake angles (from -60° to $+60^\circ$), widths of cut (1,1 to 4,34 nm), depths of cut (0,01 to 2,72 nm) and clearance angles (10° to 30°) to investigate the nature of material removal and surface generation process in ultraprecision machining and grinding. The observed material removal mechanisms can be divided into four components: (1) compression of the work material ahead of the tools; (2) chip formation akin to an extrusion-like process; (3) side flow; and (4) subsurface deformation in the machined surface. Significant volume changes (from 18,38 to 14,19 Angstrom), resulting in a densification of about 23% occur owing to phase transition from a diamond cubic (or alpha-silicon) to a beta (or beta-tin structure) in the case of machining silicon. The extent of structural changes and their contributions to each of the four material removal mechanisms depend on the tool rake angle and the width of cut. The ratio of the width of cut to depth of cut (w/d ratio) is the primary factor affecting the extent of side flow and subsurface compression. The tool rake angle and the w/d ratio are found to be dominant factors affecting the chip flow and shear zone compression ahead of the tool. Subsurface or near-surface deformation was observed with all rake angles and all cut depths down to 0.01 nm, indicating the need for an alternate final polishing process.

The papers [74; 75; 77; 80; 81; 83–87; 96; 97] deal with an investigation of the effect of crystallographic orientation and process parameters on the surface integrity of brittle semiconductor crystals in ultrapre-

cision diamond turning. The crystallographic anisotropy causes nonuniformity of the finished surface texture, microfracture topography and brittle-ductile transition boundary conditions. Specifically, in machining of silicon wafers [77], a ductile-regime was achieved along the $\langle 110 \rangle$ directions when the maximum chip thickness of less than $0,5 \mu\text{m}$. Machining conditions that formed thicker chips led to pitting, microcracks and slip lines. Such defects, which could be more than $1 \mu\text{m}$ deep, were found along the $\langle 110 \rangle$ directions and occasionally along the $\langle 100 \rangle$ directions. The test results during ductile removal in silicon [98] show that the critical chip thickness and thrust force do vary with crystallographic orientation on the cubic face. The critical chip thickness is found to be a maximum of $0,4 \mu\text{m}$ along the $\langle 100 \rangle$ cutting direction and a minimum of $0,1 \mu\text{m}$ in the $\langle 110 \rangle$ cutting direction with a -45° rake tool. Fig. 7, *a*, *b* evidently demonstrates the effect of crystallographic orientation on vastly different cracks initiation along different plunge-cut direction [97].

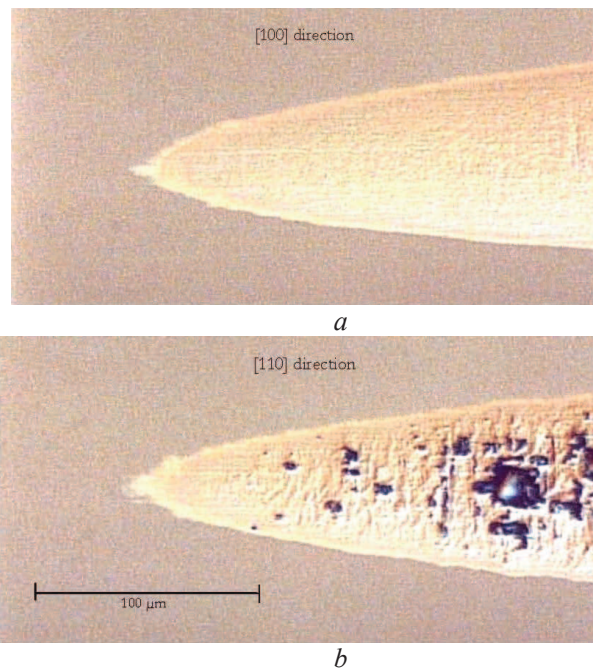


Fig. 7. Micrographs of two Si plunge-cuts [97]: The top cut (*a*) is in the $\langle 100 \rangle$ direction and the bottom (*b*) is in the $\langle 110 \rangle$ direction

Few studies [67; 68; 75] pay attention to the thermal phenomena during ductile mode cutting. The numerical results in [68] indicate that, as the cutting speed increases, thermal effects become more and more dominant and the inelastic deformation of silicon nitride will be primarily due to thermal softening. The results of [75] indicate that one type of the microfractures in CaF_2 is caused by thermal effect can be completely eliminated by using appropriate geometrical parameters of the tool and cutting conditions.

The effect of lubrication was considered in the studies [49; 55; 57; 75; 98]. At scratching, a fully plastic removal of single crystal silicon below critical load for fracture is observed under pentadecane lubrication, which is quite different from that under dry sliding [49]. The almost similar results were obtained by tribological experiments [55; 57]. The critical conditions for microfracturing during diamond turning of CaF_2 depend strongly on the type of cutting fluid [75]. Experimental results [98] also indicate that it is possible to prolong the ductile cutting distance of single-crystal silicon by using an appropriate coolant. In general, as indicated in [99], the success of the diamond turning of silicon substrates in ductile-regime depends on optimizing the machining parameters such as feed rate, depth of cut, tool rake angles, spindle speed, the cutting lubricants and the crystallographic orientation of the crystal being cut. The fig. 8 shows the critical value of tool feed, as the example of the dependency of the increased feed rate (from left to right) on the observed pitting of the Si machined surface.

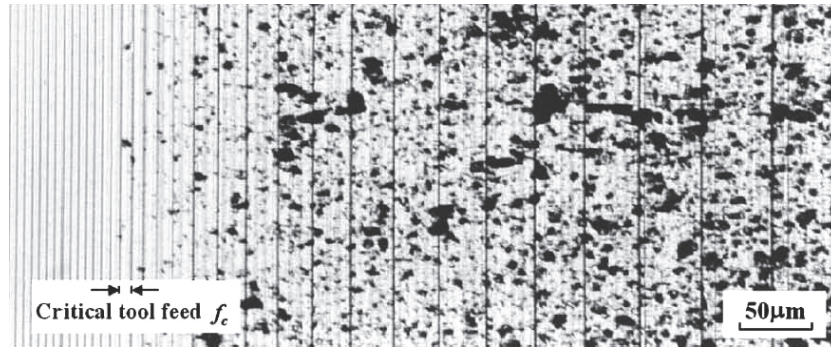


Fig. 8. Micrograph of machined surface of silicon when feed rate was increased from left to right affecting the pitting [106]

The simulation approach [67; 86; 87] could successfully explain existing experimental phenomena, support the determination of the cutting

conditions and to be helpful for optimizing tool geometry design in silicon machining without resorting to trial and error. However, to gain the real practical results, many experimental studies [38; 66; 75; 96; 100] were carried out to provide a means for the optimization of the tool design and to find the optimum cutting conditions for obtaining ductile regime.

The fundamental obstacle for industrial application of ductile regime turning of brittle material is diamond tool wear and its effect on chip formation mode. It was found in [98] that the tool wear could be generally classified into two types: micro-chippings and gradual wear, the predominant wear mechanism depending on undeformed chip thickness. In ductile mode cutting, flank wear was predominant and the flank wear land was characterized by trailing micro-grooves and step structures. The tool wear causes micro-fracturing on machined surface, yields discontinuous chips and raises cutting forces and force ratio. The main cutting edge of an unused single crystal diamond tool, as well after brittle and ductile mode Si cutting are shown in fig. 9. Experimental results in [101; 102] also indicated that wear occurred mainly on the flank face of the tool and the wear pattern was typically mechanical abrasive wear, adhesive wear and possible nano-chemical wear. At higher cutting distance, crater wear with small grooves in the vicinity of cutting edge was observed on the tool rake face. In the study [103], the variation of the tool shape and cutting edge radius due to tool wear and its influence on the nanoscale ductile mode cutting of silicon wafer with single crystalline diamond tools is investigated and analyzed. It was found that the tool cutting edges undergo two processes simultaneously. One is the wear of material on the tool main cutting edge, which increases the main cutting edge radius, but leaves the shape of the main cutting edge unchanged, enhancing the conditions for ductile mode chip formation.

The other one is the generation of nano or micro grooves at the tool flank, which forms sub-cutting edges of much smaller radii on the main cutting edge. As the grooves become deeper and deeper, the sub-cutting edges extend towards the tool rake face ultimately becoming the dominating cutting edge of much smaller radius. In such a way, these sub-cutting edges tend to change the cutting mode from ductile to brittle. The modeling by the finite element approach [67] states that as the edge radius is beyond a critical value (similar to 200 nm), the primary high-temperature zone shifts from the rake face side to the flank face side, causing a transition in the tool wear pattern from crater wear to flank wear.

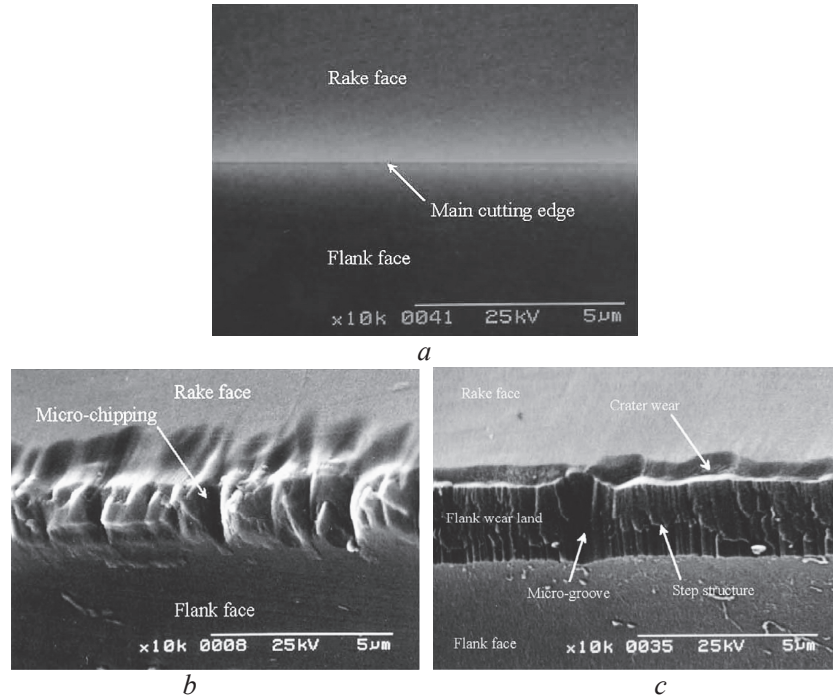


Fig. 9. SEM photographs of the main cutting edge of an unused single crystal diamond tool (a), after brittle mode cutting showing occurrence of micro-chippings (b) and after ductile mode cutting showing the changes of crater wear and flank wear land (c) [98]

A series of screening experiments were conducted, as described in [104], to survey the influence of machining parameters on tool wear during ductile regime diamond turning of large single-crystal silicon. The machining parameters under investigation were depth-of-cut, feed rate, surface cutting speed, tool radius, tool rake angle and side rake angle, and cutting fluid. It was found that track length, chip size, tool rake angle and surface cutting speed significantly affect tool wear, while cutting fluid and side rake angle do not significantly affect tool wear within the ranges tested. The track length, or machining distance, is the single most influential characteristic that causes tool wear. For a fixed part area, a decrease in track length corresponds to an increase in feed rate. Less tool wear occurred on experiments with negative rake angle tools, larger chip sizes and higher surface velocities. The most significant re-

sult [105] whilst turning silicon showed the performance of one particular tool was consistently superior when compared with other diamond tools of the same specification. Another significant result was associated with coolant cutting fluid type. In all cases, tool life was prolonged by as much as 300% by using a specific fluid type. As [106] reports, the problem of diamond tool wear is difficult to solve for existing methods of turning with round-nosed tools due to limitation on tool feed. In the paper [106], ductile regime turning using the straight-nosed diamond tool was proposed. This method enables thinning of undeformed chip thickness in the nanometric range and at the same time provides significant cutting width ensuring plain strain conditions. Adopting a small cutting edge angle enables ductile regime turning at a large tool feed up to a few tens of micrometers.

As it is well known, single crystal diamond possesses strong anisotropy. Its mechanical and physical properties vary with crystallographic orientation. In the studies [101; 102; 107], the wear characteristics of single point diamond tools and the effect of diamond crystallographic orientation were investigated on nano-scale ductile cutting of silicon. The machining data show [101] that wear resistance of the tool and tool life were greater when the crystallographic orientation of the rake face was $\langle 110 \rangle$ than when it was $\langle 100 \rangle$ or $\langle 111 \rangle$. The thrust force on the diamond tool was lower when the rake face crystallographic orientation was $\langle 110 \rangle$ than when it was some other orientation. For all the crystallographic orientations studied in the diamond tools, gradual tool flank wear had no significant effect on the surface roughness of machined silicon work material. From the other study [102], it is found that in terms of tool flank wear resistance, the tool life of the diamond cutter with crystal orientations $\langle 100 \rangle$ as the rake and $\langle 110 \rangle$ as the flank planes, was much longer than those of the diamond cutters with other crystal orientations as the rake and flank planes. As it was observed in [107] that under certain crystalline orientations of the diamond tool, such as with $\langle 110 \rangle$ or $\langle 100 \rangle$ for the tool rake face, good integrity of the machined surface could be generated. However, when the tool had the $\langle 111 \rangle$ orientation for the rake face, the machined surface was fractured. The effect of diamond crystalline orientations on the machined surface were experimentally investigated using the $\langle 100 \rangle$, $\langle 110 \rangle$, and $\langle 111 \rangle$ orientations for the rake faces of single-crystal diamond tools. The re-

sults showed that when the rake face orientation of the diamond cutter was changed from $\langle 100 \rangle$ or $\langle 110 \rangle$ to $\langle 111 \rangle$, the chip formation mode changed from ductile to brittle. The cause of such behavior of single-crystal diamond tools was found to be the different values of the Young's modulus of single-crystal diamond in the $\langle 100 \rangle$, $\langle 110 \rangle$, and $\langle 111 \rangle$ orientations.

In the studies [108; 109], the mechanism of the groove wear in nanoscale ductile mode cutting of monocrystalline silicon by diamond is investigated by molecular dynamics simulation of the cutting process. The results show that the temperature rise in the chip formation zone could soften the material at the flank face of the diamond cutting tool. Also, the high hydrostatic pressure in the chip formation region could result in the work-piece material phase transformation from monocrystalline to amorphous, in which the material interatomic bond length varies, yielding atom groups of much shorter bond lengths. Such atom groups could be many times harder than that of the original monocrystalline silicon and could act as «dynamic hard particles» in the material. Having the dynamic hard particles ploughing on the softened flank face of the diamond tool, the micro/nano grooves could be formed, yielding the micro/nano groove wear as observed.

Laser micromachining has proven to be a very successful tool for precision machining and microfabrication with applications in many advanced fields. The paper [110] describe as diamond-machined silicon wafers have been irradiated by a nanosecond pulsed Nd:YAG laser. The results indicate that at specific laser energy intensity levels, the machining-induced subsurface damage layer of silicon has been reconstructed to a perfect single-crystalline structure identical to the bulk. Laser irradiation causes two effects on silicon; one is the epitaxial regrowth of the near-surface amorphous layer, and the other is the complete removal of the dislocations from the crystalline layer. It is the dislocation-free crystalline region that serves as the seed layer to recrystallize the amorphous layer, enabling excellent crystalline perfection. The authors claim that these findings may offer practical alternatives to current chemo-mechanical processing methods for silicon wafers.

To augment the ductile regime machining of nominally brittle materials, the high-pressure phase can be preferentially heated and thermally softened by using concentrated energy sources such as laser beams [111; 112]. It was found in [113; 114] that laser machining of

silicon wafers has induced tensile stress in the range 0,8-2,0 GPa. The machining process has also led to the creation of up to 20% amorphous silicon in the machined area. In the research [115], the effect of the pressure and temperature and the interactions of these two factors on the micro-laser assisted machining process are studied by using a hybrid machining system that consists of a diamond stylus and infrared fiber laser heating source. The increased ductility of the material was achieved by the laser heating and respective thermal softening. Notably, the results of scratch tests show a doubling of the scratch depth which suggests a ~50% reduction of hardness due to thermal softening.

It should be noted to conclude this survey that dissertations [86; 97; 111; 116–118] also include extended reviews of ductile mode machining, however they are oriented on the particular goals of the theses.

CONCLUSION: The above reviewed papers designate the values of the tool cutting edge radius, depth of cut, undeformed chip thickness, tool rake angles as the critical for maintaining the ductile mode. These parameters are affected by crystallographic orientation of the workpiece and diamond tool, as well as type of cutting lubricants. The machining parameters (feed rate, spindle speed, cutting speed, etc.) as well should be optimized.

References

1. King R. F. *et al.* (1954) Proc of Roy Soc of London, Ser A **223**: 225.
2. Huerta M. *et al.* (1976) ASME Trans, J Eng Ind **98**: 459.
3. Ngoi B.K. *et al.* (2000) Int J Adv Man Tech **16**(8): 547.
4. Zhong Z.W. (2003) Int J Adv Manuf Tech **21**(8): 579.
5. Pei Z.J. *et al.* (1999) Int J Mach Tools & Man **39**(7): 1103.
6. Pei Z.J. *et al.* (2001). Int J Mach Tools & Man **41**(5): 659.
7. Stephenson D.J. (2006) Adv in Tech Mat & Mat Proc **8**(1): 13.
8. Gogotsi Y. *et al.* (1999) Sem Sci & Tech **14**(10): 936.
9. Koinkar V. N. *et al.* (1997). J Mat Res **12**(12): 3219.
10. Kunz R.R. *et al.* (1996). J Mat Res **11**(5): 1228.
11. Young H.T. *et al.* (2006) Int J Adv Manuf Tech **29**: 372.
12. Patten J. *et al.* (2005) J Manuf Sci & Eng-Trans ASME **127**(3): 522.
13. Yin L. *et al.* (2003) Adv Abr Tech **238**(2): 59.
14. Bifano T. *et al.* (1994) Prec Eng-J Am Soc Prec Eng **16**(2): 109.
15. Hung N.P. *et al.* (1999) Mach Sci & Tech **3**(2): 255.
16. Yan J. *et al.* (2003) Adv Abr Tech **238**(2): 43.
17. Yan J.W. *et al.* (2005) J Mic & Mic **15**(10): 1925.
18. Yoshino M. *et al.* (2005) J Man Sci & Eng-Trans ASME **127**(4): 837.

19. Venkatesh V.C. (2003) Curr Sci **84**(9): 1211.
20. Demirci I. *et al.* (2010) J Mat Proc Tech **210**(3): 4.66.
21. Bandyopadhyay B.P. *et al.* (1996) Mat & Man Proc **11**(5): 789.
22. Bandyopadhyay B.P. *et al.* (1999) Int J Mach Tools & Manuf **39**(5): 839.
23. Sun Y.L. *et al.* (2007) Chinese J Chem Phys **20**(6): 643.
24. Zuo D.W. *et al.* (2009) J Vac Sci & Tech B **27**(3): 1514.
25. Domnich V. *et al.* (2002) Rev Adv Mater Sci **3**: 1.
26. Morris J.C. *et al.* (1995) J Am Cer Soc **78**(8): 2015.
27. Puttick K.E. *et al.* (1995) Trib Int **28**(6): 349.
28. Yan J.W. *et al.* (2005) Appl Phys Let **86**(18): 1, No 181913.
29. Yan J.W. *et al.* (2005) Appl Phys Let **87**(21): 1, No 211901.
30. Yan J.W. *et al.* (2006) Mat Sci & Eng A **423**(1–2): 19.
31. Tanikella B.V. *et al.* (1996) Appl Phys Let **69**(19): 2870.
32. Pizani P.S. *et al.* (2000) **87**(3): 1280.
33. Yan J.W. (2004) J Appl Phys **95**(4): 2094.
34. Jasinevicius R.G. *et al.* (2005) J Braz Soc Mech Sci & Eng **XXVII** (4): 440.
35. Jasinevicius R.G. *et al.* (2007) J Braz Soc Mech Sci & Eng **XXIX** (1): 49.
36. Jasinevicius R.G. *et al.* (2007) Int J Adv Man Tech **34**: 680.
37. Jasinevicius R.G. *et al.* (2007) Sem Sci & Tech **22**(5): 561.
38. Jasinevicius R.G. *et al.* (2008) Proc Ins Mec Eng Pt B **222**(9): 1065.
39. Chung K.H. *et al.* (2005) Ultramicroscopy **102**(2): 161.
40. Kim H.J. *et al.* (2009) IEEE Trans on Magn **45**(5): 2328.
41. Gogotsi Y. *et al.* (2001) Sem Sci & Tech **16**(5): 345.
42. Zhou M. *et al.* (2001) Mat & Man Proc **16**(4): 447.
43. Patten J.A. *et al.* (2007) Sem Mach Micro-Nano Scale: ISBN: 978-81-7895-301-4, 1–36.
44. Zhao X.Z. *et al.* (1998) Wear **223**(1-2): 66.
45. Youn S.W. *et al.* (2004) Mat Sci & Eng A **384**(1–2): 275.
46. Koshimizu S. *et al.* (2001) Mach Sci & Tech **5**(1): 101.
47. Bhattacharya B. *et al.* (2007) Int J Mach & Mach Mat **2**(1): 17.
48. Dong L. *et al.* (2005) Int J Man Tech & Man **7**(5–6): 530.
49. Li X.C. *et al.* (2007) Trib Int **40**(2): 360.
50. Park J.W. *et al.* (2007) J Mat Proc Tech **187**: 321.
51. Yu B. *et al.* (2009) Nanotechnology **20**(46): No 465303.
52. Brinksmeier E. *et al.* (1998) Proc ASPE 1998 Spr Topl Meet **17**: 55.
53. Abdel-Aal H. A. *et al.* (2005) Wear **259**: 1343.
54. Abdel-Aal H. A. *et al.* (2006) Mat Char **57**(4–5): 281.
55. Kovalchenko A. *et al.* (2002) Trib Trans **45**(3): 372.
56. Li X.C. *et al.* (2008) Trib Int **41**(3): 189.

57. *Li X. et al.* (2006) Trib Let **24**(1): 61.
58. *Li X.C. et al.* (2009) Trib Int **42**(5): 628.
59. *Cai M.B. et al.* (2007) Proc Inst Mech Eng Pt B **221**: 1511.
60. *Han X.S. et al.* (2008) Eur Phys J-Appl Phys **42**(3): 255.
61. *Tang Q.H. et al.* (2006) J Phys D-Appl Phys **39**(16): 3674.
62. *Tang Y.L. et al.* (2006) Adv in Mach & Man Tech **315-316**: 792.
63. *Wu H. et al.* (2004) Adv Mat Man Sci &Tech **471-472**: 144.
64. *Liu K. et al.* (2004) SIMTech Technical Report: 101.
65. *Jasinevicius R.G.* (2006) J Mat Proc Tech **179**(1-3): 111.
66. *Jasinevicius R.G. et al.* (2000) J Non-Crys Sol **272**(2-3): 174.
67. *Yan J.W. et al.* (2009) Sem Sci & Tech **24**(7): No 075018.
68. *Ajjarapu S.K. et al.* (2004) Proc Instn Mech Eng C **218**(6): 577.
69. *Tanaka H. et al.* (2004) Proc. Instn Mech Eng Pt C **218**(6): 583.
70. *Tanaka H. et al.* (2007) Cirp Annals-Man Tech **56**(1): 53.
71. *Cai M. et al.* (2007) Int J Comp Appl in Tech **28**(1): 2.
72. *Yan J.W. et al.* (2009) Prec Eng **33**(4): 378.
73. *Yan J.W. et al.* (2009) J Nanosci & Nanotech **9**(2): 1423.
74. *Yan J.W. et al.* (2006) JSME Int J Pt C **49**(1): 63.
75. *Yan J. et al.* (2004) Int J Adv Man Tech **24**(9-10): 640.
76. *Egashira K. et al.* (2002) Prec Eng **26**(3): 263.
77. *Hung N.P. et al.* (2000) Int J Adv Man Tech **16**(12): 871.
78. *Li X.P. et al.* (2010) Int J Adv Man Tech **48**(9-12): 993.
79. *Blake P. N. et al.* (1990) J Am Cer Soc **73**(4): 949.
80. *Young H.T. et al.* (2006) Prog Adv Manuf M/N Tech Pt 1&2 **505-7**: 253.
81. *Young H.T. et al.* (2007) J Mat Proc Tech **182**(1-3): 157-162.
82. *Bhattacharya B. et al.* (2006) ASME Int Conf Manuf Sci & Eng, Ypsilanti, MI, USA.
83. *O'Connor B.P. et al.* (2005) Prec Eng-J Int Soc Prec Eng **29**(1): 124.
84. *Yan J.W. et al.* (2004) JSME Int J Pt C **47**(1): 29.
85. *Yan J.W. et al.* (2004) J Vac Sci & Tech B **22**(1): 46-51.
86. *Venkatachalam S.* (2007) PhD Dissertation, Georgia Tech, Atlanta, USA.
87. *Venkatachalam S. et al.* (2009) J Mat Proc Tech **209**(7): 3306.
88. *Rusnaldy T.J. et al.* (2007) Int J Mach Tools & Manuf **47**: 2111.
89. *Fang F.Z. et al.* (2007) J Mat Proc Tech **184**(1-3): 407.
90. *Liu K. et al.* (2001) Trans. NAMRI/SME **29**: 251.
91. *Arefin S. et al.* (2007) Proc Inst Mech Eng Pt B-J Eng Man **221**(2): 213.
92. *Arefin S. et al.* (2007) Int J Adv Man Tech **31**(7-8): 655.
93. *Cai M.B. et al.* (2007) Int J Mach Tools & Manuf **47**(1): 75.
94. *Cai M.B. et al.* (2007) Int J Mach Tools & Manuf **47**(3-4): 562.
95. *Komanduri R. et al.* (2001) Phil Mag Pt B **81**(12): 1989.
96. *Cheung C.F. et al.* (2002) Mat & Manuf Proc **17**(2): 251.
97. *O'Connor B.P.* (2002) Thesis of Master of Sci, Penn State Univ, PA, USA.

98. Yan J.W. et al. (2003) Wear **255**(7–12): 1380.
99. Leung T.P. et al. (1998) J Mat Proc Tech **73**(1–3): 42.
100. Rusnaldy T.J. et al. (2008) Int J Adv Man Tech **39**(1–2): 85.
101. Uddin M.S. et al. (2004) Wear **257**(7–8): 751.
102. Uddin M.S. et al. (2007) J Mat Proc Tech **185**(1–3): 24.
103. Li X.P. et al. (2005) Wear **259**(7–12): 1207.
104. Born D.K. (2001) Prec Eng **25**(4): 247.
105. Durazo-Cardenas I. et al. (2007) Wear **262**(3–4): 340.
106. Yan J.W. et al. (2002) J Mat Proc Tech **121**(2–3): 363.
107. Li X.P. et al. (2008) Proc Inst Mech Eng Pt B (12): 1597.
108. Cai M.B. et al. (2007) Wear **263**(7–12): 1459.
109. Cai M.B. et al. (2007) J Man Sci & Eng-Trans ASME **129**(2): 281.
110. Yan J. et al. (2007) Sem Sci & Tech **22**(4): 392.
111. Dong L. (2006) PhD dissertation. Univ of North Carolina at Charlotte, NC, USA.
112. Dong L. et al. (2007) Adv Laser Appl Conf & Expo, Sept. 24-25, Boston.
113. Amer M.S. et al. (2002) Appl Surf Sci **187**(3–4): 291.
114. Amer M.S. et al. (2005) Appl Surf Sci **242**: 162.
115. Shayan A.R. et al. (2009) Trans NAMRI/SME **37**: 75.
116. Islam M.M. (2005) Thesis of Master of Engineering, Dep of Mech Eng, National University of Singapore.
117. Abdur-Rasheed A. (2007) Dissertation of Master of Manufacturing Engineering, Kulliyah of Engineering Int Islamic University, Malaysia.
118. Javvaji R. (2008) Thesis of Master of Engineering, Dep of Mech Eng, National University of Singapore.

Ковальченко А.М. Огляд досліджень в області в'язкого режиму обробки напівпровідників, кераміки та скла // Проблеми тертя та зношування: наук.-техн. зб. – К.: НАУ, 2012. – Вип. 57. – С.5–33.

Огляд присвячений актуальному методу в'язкого режиму обробки крихких матеріалів, таких як напівпровідники, кераміка і скло для отримання гладкої і бездефектної поверхні. В'язкий режим пов'язаний із здійсненням фазових перетворень (металізацією або аморфізацією), які мають місце в крихких матеріалах під дією контактної навантаження, яким може бути ідентування, дряпання, тертя, шліфування і різання. Огляд розглядає теоретичні та експериментальні дослідження. Показано, що радіус ріжучої кромки, глибина різання, недеформована товщина стружки, кут нахилу різця, кристалографічна орієнтація, тип мастильної рідини і деякі інші параметри є критичними для реалізації в'язкого режиму різання.

Рис. 9, список літ.: 118 найм.

Ковальченко А.М. Обзор исследований в области вязкого режима обработки полупроводников, керамики и стекла

Обзор посвящён актуальному методу вязкого режима обработки хрупких материалов, таких как полупроводники, керамика и стекло для получения гладкой и бездефектной поверхности. Вязкий режим связан с осуществлением фазовых превращений (металлизацией или аморфизацией), которые имеют место в хрупких материалах под действием контактного нагружения, каким может быть индентирование, царапание, трение, шлифование и резание. Обзор рассматривает теоретические и экспериментальные исследования. Показано, что радиус режущей кромки, глубина резания, недеформируемая толщина стружки, угол наклона резца, кристаллографическая ориентация, тип смазочной жидкости и некоторые другие параметры являются критическими для реализации вязкого режима резания.

Стаття надійшла до редакції 10.01.2012